A hierarchy of dynamic equations for solid isotropic micropolar circular cylinders

A hierarchy of dynamic equations for solid isotropic micropolar circular cylinders

Hossein Abadikhah, Peter D. Folkow*

Department of Applied Mechanics, Chalmers University of Technology, SE-412 96 Göteborg, Sweden

Abstract

This work considers the derivation procedure and evaluation of dynamic equations for isotropic micropolar circular cylinders by adopting a power series expansion method in the radial coordinate. Variationally consistent equations of motion together with pertinent sets of boundary conditions are expressed in a systematic fashion up to arbitrary order. The numerical results cover eigenfrequencies, mode shapes and field distributions over cross sections for axisymmetric and flexural motion adopting different sets of end boundary conditions for equations of different truncation orders of the present method. The results illustrate that the present approach may render benchmark solutions provided that higher order equations are used, and act as accurate approximate engineering solution for lower order equations.

Keywords: Micropolar, Series expansion, Cylinder, Beam, Eigenfrequency, Benchmark

1. Introduction

Outside the realm of classical materials there exists a range of materials which posses internal microstructure; such materials often have granular or

*Corresponding author. Tel: +46 31 7721521, Fax: +46 31 772 3827.

Email addresses: hossein.abadikhah@chalmers.se (Hossein Abadikhah), peter.folkow@chalmers.se (Peter D. Folkow)

fibrous structure. In classical elasticity theory, the effects of such microstructures are not considered which results in incorrect predictions in relations to experiments. A main source for this shortcoming is that the classical models of elasticity assume that particles interact only through the action of a force vector. Hereby, the classical theories fail to account for the internal microstructure. In order to remedy the disparity between theory and experiment it is suggested that interaction between particles could be through both a force and a moment vector. This is the basis for the theory developed by the Cosserat brothers [1] which was later developed to other theories including the theory of micropolar elasticity due to Eringen [2]. Eringen developed a consistent theory where both equations of motions as well as constitutive equations are derived systematically for micropolar materials. The main difference between the theory of micropolar elasticity and classical elasticity is the types of degrees of freedom each point in a material exhibit. In classical elasticity the position and orientation of each material point is described by three translational degrees of freedom. However, in micropolar elasticity each point is described by six degrees of freedom: three translational and three rotational. In essence, each material point is considered to be a rigid body. The underlining assumptions of micropolar elasticity result in an extension of the regular Cauchy stress tensor, where the micropolar stress tensor is generally nonsymmetric. As a direct consequence of the rotational degrees of freedom, micropolar elasticity also introduces the nonsymmetric couple stress tensor.

Since the development of micropolar elasticity theory many structural geometries have been studied, in particular plates and shells. However, micropolar cylinders are studied sparsely and only for certain cases.

The majority of studies on micropolar cylinders are for static cases. Ieşan [3] considers static solution for the isotropic bars in torsion while Krishna Reddy and Venkatasubramanian [4, 5] deal with St. Venant's problem and flexural rigidity for circular cylinders, respectively. More recently Taliercio and Veber [6, 7] study the special cases of an orthotropic micropolar cylinder subjected to a uniform internal or external pressure and also the case where the orthotropic cylinder is subjected to torsion. FE solutions for straight and curved beams are studied in [8]. Moreover, the extended case of chiral effects in micropolar cylinders have also been studied [9, 10].

As for dynamical effects in micropolar cylinders Smith [11] and Willson [12]

derived analytic dispersion equations for an isotropic cylinder subjected to axisymmetric and torsional motion. Vasudeva and Bhaskara [13] studied the frequency equations to any mode (extensional, torsional and flexural) using asymptotic theory, and later for three dimensional theory [14]. More recently, Marin and Baleanu consider vibrational effects in micropolar thermoelastic cylinders [15]. Studies on various Timoshenko like micropolar beam equations for rectangular cross section have been developed [16, 17, 18]. Among these Ramezani et al. [17] adopt a more general series expansion approach. A mathematical approach for deriving static torsional and Timoshenko like models based on asymptotic theories is given in [19], while [20] studies a non-local micropolar Timoshenko beam theory.

The present method of deriving approximate equations for different types of structural elements is based on the works of Boström et al. [21], for an isotropic plate. The method has also been employed for plates that are anisotropic [22], porous [23] and functionally graded [24]. Abadikhah and Folkow have also here studied plates that are micropolar [25] and micropolar functionally graded [26]. Approximate equations for isotropic and anisotropic functionally graded cylindrical shells are also constructed using the present method [27, 28]. Concerning the case of solid circular cylinders, Boström [29] derived approximate equations and studied the special case of axisymmetric extensional motion. Folkow and Mauritsson [30] generalized the procedure for obtaining approximate cylinder equations for axisymmetric extensional motion and developed a variationally systematic approach for deriving end conditions. This work was extended by Abadikhah and Folkow [31] to encompass all displacement families; among them axisymmetric extensional, torsional and flexural motion.

The present paper systematically derives a hierarchy of approximate dynamical equations for a solid isotropic micropolar circular cylinder to an arbitrary order for various mode families (axisymmetric extensional, torsional, flexural). Appropriate end conditions are also derived in a systematic and variationally consistent manner to the desired order. This enables the derivation and solution of static and dynamic field equations for each of these mode families (axisymmetric, torsional, flexural) in a systematic manner for a range of various lateral and end boundary conditions. By varying the truncation order, the lower order sets may be used as simple engineering equations, while higher order sets may be used for benchmark solutions to three dimensional micropolar cylinder problems.

In the present method, the displacement and micro-rotation field are expanded in a Fourier series in the circumferential coordinate as well as a power series in the radial coordinate. As a consequence, the stress and couple stress tensors are obtained in a similar manner. Recursion relations are constructed from the three dimensional micropolar equations of motion, where all higher order expansion functions of each field can be written in terms of a finite set of lower order expansion functions without any truncations. The lateral boundary conditions are stated at the radial surface of the cylinder; these are the approximate micropolar cylinder equations. Hereby, the boundary conditions are exactly fulfilled no matter the truncation order. In order to derive the set of possible end conditions a variational calculus approach is used [31]. The approximate micropolar cylinder equations are evaluated through a study of eigenfrequencies, mode shapes and stress distributions.

2. Theory of linear micropolar elasticity

Consider a micropolar continuum where the field variables are expressed in Cartesian coordinates. In the absence of body forces and body couples, the equations of balance of momentum and moment of momentum are written as [2]

$$t_{kl,k} = \rho \ddot{u}_l, \tag{1}$$

$$m_{kl,k} + \epsilon_{lkm} t_{km} = \rho j_{lk} \ddot{\phi}_k, \tag{2}$$

where t_{kl} is the stress tensor, m_{kl} is the couple stress tensor, u_l is the displacement vector, ϕ_k is the micro-rotation vector, ρ is the density, j_{lk} is the microinertia tensor and ϵ_{lkm} is the permutation symbol. Indices that follow a comma indicate partial differentiation. The tractions are defined in accordance to

$$t_l = t_{kl} n_k, \tag{3}$$

$$m_l = m_{kl} n_k, \tag{4}$$

where n_k is an outward pointing normal. Supplementing the equations of motion, two constitutive relations for the stress and couple stress are needed. For a homogenous and isotropic material the constitutive relations are given

by [2]

$$t_{kl} = \lambda \varepsilon_{mm} \delta_{kl} + (\mu + \kappa) \varepsilon_{kl} + \mu \varepsilon_{lk}, \tag{5}$$

$$m_{kl} = \alpha \gamma_{mm} \delta_{kl} + \beta \gamma_{kl} + \gamma \gamma_{lk}, \tag{6}$$

where δ_{kl} is the Kronecker delta, λ and μ are Lamé parameters while α, β, γ and κ are micropolar elastic moduli. For spin-isotropic materials the microinertia reduces to a scalar quantity, $j_{kl} = j\delta_{kl}$. Moreover the micropolar strain tensors ε_{kl} and γ_{kl} are defined as [2]

$$\varepsilon_{kl} = u_{l,k} + \epsilon_{lkm} \phi_m, \tag{7}$$

$$\gamma_{kl} = \phi_{k,l}. \tag{8}$$

3. Series expansion, stresses and recursion relations

3.1. Series expansion

Consider a circular cylinder with length L and radius a. The cylinder is micropolar, homogenous, isotropic and linearly elastic. Cylindrical coordinates are used with radial coordinate r, circumferential coordinate θ and longitudinal coordinate z. The corresponding radial, circumferential and longitudinal displacement and micro-rotation fields are denoted u, v, w, ϕ, χ and ψ.

In order to derive the set of micropolar cylinder equations, the displacement fields and micro-rotation fields are expanded both as a Fourier series in the circumferential coordinate θ and as a power series in the radial coordinate r

[29, 30, 31]:

$$
\begin{aligned}
u &= \sum_{m=0}^{\infty} \tilde{u}_m(r,z,t)\cos(m\theta) = \sum_{m=0}^{\infty}\sum_{k=0}^{\infty} r^{m+2k-1} u_{m+2k-1,m}(z,t)\cos(m\theta),\\
v &= \sum_{m=0}^{\infty} \tilde{v}_m(r,z,t)\sin(m\theta) = \sum_{m=0}^{\infty}\sum_{k=0}^{\infty} r^{m+2k-1} v_{m+2k-1,m}(z,t)\sin(m\theta),\\
w &= \sum_{m=0}^{\infty} \tilde{w}_m(r,z,t)\cos(m\theta) = \sum_{m=0}^{\infty}\sum_{k=0}^{\infty} r^{m+2k} w_{m+2k,m}(z,t)\cos(m\theta), \quad (9)\\
\phi &= \sum_{m=0}^{\infty} \tilde{\phi}_m(r,z,t)\sin(m\theta) = \sum_{m=0}^{\infty}\sum_{k=0}^{\infty} r^{m+2k-1} \phi_{m+2k-1,m}(z,t)\sin(m\theta),\\
\chi &= \sum_{m=0}^{\infty} \tilde{\chi}_m(r,z,t)\cos(m\theta) = \sum_{m=0}^{\infty}\sum_{k=0}^{\infty} r^{m+2k-1} \chi_{m+2k-1,m}(z,t)\cos(m\theta),\\
\psi &= \sum_{m=0}^{\infty} \tilde{\psi}_m(r,z,t)\sin(m\theta) = \sum_{m=0}^{\infty}\sum_{k=0}^{\infty} r^{m+2k} \psi_{m+2k,m}(z,t)\sin(m\theta).
\end{aligned}
$$

Note the new definition of the two indices for the expansion function $u_{i,j}(z,t)$ etc. The first index is the order of the radial series expansion and the second one is the Fourier mode. Here the angle θ is measured from a vertical axis in a plane through the cross section of the cylinder with a horizontal axis [32]. By choosing the Fourier mode $m = 0$, the axisymmetric case is obtained. The pure torsional case is simply obtained by interchanging the cosine and sine dependency in Eq. (9) for $m = 0$.

Studying the ansatz Eq. (9), one can deduce that the expansion functions for the displacement and micro-rotations start at the indices $m-1$ or m and subsequent indices increase by two. This particular case can be derived by assuming a complete power series expansion including all expansion functions and the equations for micropolar theory Eqs. (1)–(2) and Eqs. (5)–(6).

3.2. Stresses

In the previous Section 3.1 the series expansions of the displacements and micro-rotations and the corresponding expansion functions are introduced. By using the ansatz Eq. (9) into the constitutive relations Eqs. (5)–(6) together with the strain expressions Eqs. (7)–(8), it is possible to express

both the stress tensor and the couple stress tensor as power series expansion in the radial coordinate for each Fourier mode. For the sake of brevity the symbol σ_{kl} will be used to both denote the stress tensor t_{kl} and the couple stress tensor m_{kl}. Hereby the total stress tensor, either the regular stress tensor or the couple stress tensor, are written in a similar manner as the displacements in Eq. (9), that is

$$\sigma_{kl} = \sum_{m=0}^{\infty} \tilde{\sigma}_{kl,\{m\}}(r,z,t)\{\cos(m\theta);\sin(m\theta)\}, \tag{10}$$

where

$$\begin{aligned} \tilde{\sigma}_{ab,\{m\}} &= r^{m-2}\sigma_{ab,\{m-2,m\}} + r^{m}\sigma_{ab,\{m,m\}} + r^{m+2}\sigma_{ab,\{m+2,m\}} + \ldots, \\ \tilde{\sigma}_{cd,\{m\}} &= r^{m-1}\sigma_{cd,\{m-1,m\}} + r^{m+1}\sigma_{cd,\{m+1,m\}} + r^{m+3}\sigma_{cd,\{m+3,m\}} + \ldots. \end{aligned} \tag{11}$$

Here ab is for $\{rr, \theta\theta, zz, r\theta, \theta r\}$ and cd is for $\{\theta z, z\theta, rz, zr\}$ where the bracketed indices are the radial order and the Fourier mode, respectively. The circumferential dependency $\cos(m\theta)$ or $\sin(m\theta)$ used for each stress component in Eq. (10) follows directly from the ansatz Eq. (9). The expression for each stress component is presented in Appendix A. Note that the stress $\sigma_{ab,\{m-2,m\}}$ and $\sigma_{cd,\{m-1,m\}}$ have negative powers of r for some values of m. This fact implies that the stress is either infinite at the origin of the cylinder or that the stress expansion functions $\sigma_{ab,\{m-2,m\}}$ and $\sigma_{cd,\{m-1,m\}}$ vanish for some Fourier modes. In Section, 3.3, the relations that cause $\sigma_{ab,\{m-2,m\}}$ and $\sigma_{cd,\{m-1,m\}}$ to vanish are discussed more in detail.

3.3. Recursion relations

At this point in the derivation procedure of the micropolar cylinder equations, the displacement and micro-rotation fields have been replaced by series expansion functions for each field. Therefore an infinite amount of unknown expansions functions need to be determined. However, there exists a linear relationship between expansions functions, which will be used to reduce the amount of unknown expansion functions to a finite set. The micropolar cylinder equations can then be used to solve for this finite set and all other expansion functions are subsequently written as a linear combination of this finite set. By inserting the series expansions of the displacements,

micro-rotations and stresses Eqs. (9)–(11) into the equations of motion Eqs. (1)–(2) and collecting terms of equal radial power, one obtains expressions relating different expansion functions [31]. The relations can be generalized in the following form for the displacement expansions

$$u_{m+k+2,m} = f_u(u_{m+k,m}, v_{m+k,m}, w_{m+k+1,m}, \phi_{m+k,m}, \chi_{m+k,m}, \psi_{m+k+1,m}), \tag{12}$$

$$v_{m+k+2,m} = f_v(u_{m+k,m}, v_{m+k,m}, w_{m+k+1,m}, \phi_{m+k,m}, \chi_{m+k,m}, \psi_{m+k+1,m}), \tag{13}$$

$$w_{m+k+2,m} = f_w(u_{m+k+1,m}, v_{m+k+1,m}, w_{m+k,m}, \phi_{m+k+1,m}, \chi_{m+k+1,m}), \tag{14}$$

and similarly for the micro-rotation expansions

$$\phi_{m+k+2,m} = f_\phi(u_{m+k,m}, v_{m+k,m}, w_{m+k+1,m}, \phi_{m+k,m}, \chi_{m+k,m}, \psi_{m+k+1,m}), \tag{15}$$

$$\chi_{m+k+2,m} = f_\chi(u_{m+k,m}, v_{m+k,m}, w_{m+k+1,m}, \phi_{m+k,m}, \chi_{m+k,m}, \psi_{m+k+1,m}), \tag{16}$$

$$\psi_{m+k+2,m} = f_\psi(u_{m+k+1,m}, v_{m+k+1,m}, \phi_{m+k+1,m}, \chi_{m+k+1,m}, \psi_{m+k,m}), \tag{17}$$

where k is even in Eqs. (14) and (17), and odd in the other in line with the ansatz in Eq. (9). The six recursions operators $\{f_u, f_v, f_w, f_\phi, f_\chi, f_\psi\}$ do not involve any approximations since they stem from the equations of motions Eqs. (1)–(2), and the power series expansion of the displacement and micro-rotation fields, Eq. (9). Furthermore, the power series have not been truncated for the derivation of the recursion relations, which is essential for the present method. The operators $\{f_u, f_v, f_w, f_\phi, f_\chi, f_\psi\}$ involve spatial and time derivatives of the expansion functions. The complete expressions of the recursion operators are presented in Appendix B.

By studying these recursion relations Eqs. (12)–(17) systematically for each term k starting from the lowest circumferential mode, it appears that some expansion functions are identically zero:

- All expansion functions where the first index is negative are identically zero.
- The expansion functions $u_{k,m}$, $v_{k,m}$, $\phi_{k,m}$ and $\chi_{k,m}$ are zero when k and m are both even or odd, respectively. The opposite is true for $w_{k,m}$ and $\psi_{k,m}$.

- All expansion functions satisfy: $u_{k,m} = v_{k,m} = \phi_{k,m} = \chi_{k,m} = w_{k,m-1} = \psi_{k,m-1} \equiv 0, \quad k < m-1.$

Note that the first constraint renders $u_{m-1,m} = v_{m-1,m} = \phi_{m-1,m} = \chi_{m-1,m} = 0$ for $m = 0$. Moreover, four further constraints are also obtained:

$$u_{m-1,m} + v_{m-1,m} = 0, \tag{18}$$

$$\phi_{m-1,m} - \chi_{m-1,m} = 0, \tag{19}$$

$$\begin{aligned} &m[(m+2)\lambda + (m+4)\mu + 2\kappa]u_{m+1,m} + m[m\lambda + (m-2)\mu - 2\kappa]v_{m+1,m} = \\ &= \rho\ddot{u}_{m-1,m} - (\mu+\kappa)u''_{m-1,m} - m(\lambda+\mu)w'_{m,m} + \kappa\chi'_{m-1,m} - m\kappa\psi_{m,m}, \end{aligned} \tag{20}$$

$$\begin{aligned} &m[2\gamma + (m+2)(\alpha+\beta)]\phi_{m+1,m} + m[2\gamma - m(\alpha+\beta)]\chi_{m+1,m} = \\ &= \rho j\ddot{\phi}_{m-1,m} - \gamma\phi''_{m-1,m} + 2\kappa\phi_{m-1,m} - m(\alpha+\beta)\psi'_{m,m} + \kappa v'_{m-1,m} + \kappa w_{m,m}. \end{aligned} \tag{21}$$

Similar constraints are also found for the classical solid isotropic cylinder case [31].

The recursion relations Eqs. (12)–(17) together with the constraint relations Eqs. (18)–(21) allow for expressing higher order index expansion functions in terms of lower order index expansion functions. This procedure will be used in the derivation process for obtaining a hierarchy of micropolar cylinder equations. The natural choice would be to use the lowest index non-zero expansion functions in line with earlier work [21]; that is $u_{m-1,m}, v_{m-1,m}, w_{m,m}, \phi_{m-1,m}, \chi_{m-1,m}$ and $\psi_{m,m}$ for $m > 0$. However due to the constraints Eqs. (18)–(19) another independent set must be opted for, which here is set to be $u_{m-1,m}, v_{m+1,m}, w_{m,m}, \phi_{m-1,m}, \chi_{m+1,m}$ and $\psi_{m,m}$ for $m > 0$. In the special case of $m = 0$, the expansion functions used for axisymmetric motion are $u_{1,0}, w_{0,0}$ and $\chi_{1,0}$, while for torsional motion the expansion functions $v_{1,0}, \phi_{1,0}$ and $\psi_{0,0}$ are used. Also note that it is the combination of these various constraints that causes the stress components $\sigma_{ab,\{m-2,m\}}$ and $\sigma_{cd,\{m-1,m\}}$ to vanish for some Fourier modes and thereby guaranteing that the stress and couple stress are not singular.

4. Cylinder equations

4.1. Lateral boundary conditions

For a cylinder governed by the equations of motion Eqs. (1) and (2), six boundary conditions must be prescribed at the surface $r = a$. These six boundary conditions are obtained by stating one field from each of the pairs $\{u, t_{rr}\}$, $\{v, t_{r\theta}\}$, $\{w, t_{rz}\}$, $\{\phi, m_{rr}\}$, $\{\chi, m_{r\theta}\}$ and $\{\psi, m_{rz}\}$. The corresponding prescribed quantity is symbolized with a hat, for instance if the radial displacement is prescribed at $r = a$, the lateral boundary condition is written as $u = \hat{u}$. Following the reasoning outlined by Abadikhah and Folkow [31] it is sufficient to prescribe the particular Fourier mode of interest. Hence, if the radial displacement mode $\tilde{u}_m(r = a, z, t)$ is chosen, the boundary conditions become $\tilde{u}_m(r = a, z, t) = \hat{u}_m$, where $\hat{u}_m$ is the m-th Fourier mode of the prescribed radial displacement.

Whether displacements, micro-rotations or traction are prescribed, one can divide all lateral boundary conditions in two categories: $m = 0$ and $m > 0$. For the case of $m = 0$, it is possible to decouple the motion into axisymmetric motion and torsional motion. The pertinent fields that can be chosen as boundary conditions are $\{u, t_{rr}\}$, $\{w, t_{rz}\}$ and $\{\chi, m_{r\theta}\}$ for the longitudinal motion and $\{v, t_{r\theta}\}$, $\{\phi, m_{rr}\}$ and $\{\psi, m_{rz}\}$ for the torsional motion, respectively. In the case $m > 0$ there is not any such decoupling possible and all six pairs must be used for selecting boundary conditions. The expressions for the m-th Fourier mode of the displacements and micro-rotations Eq. (9) as well as the stress tensors Eq. (11) are all infinite power series in terms of the radius a of the cylinder.

In practice, the set of lateral boundary conditions in power series form must be truncated. Several different truncations schemes may be adopted. The present truncation scheme amount to truncating the lateral boundary conditions in the following manner; $\{u, t_{rr}\}$, $\{v, t_{r\theta}\}$ $\{\phi, m_{rr}\}$ and $\{\chi, m_{r\theta}\}$ are truncated at $N > 1$ terms, while $\{w, t_{rz}\}$ and $\{\psi, m_{rz}\}$ are truncated at $N-1$ terms, in accordance with [31]. As mentioned in Section 3.3, all expansions functions can be written in terms of the lowest order expansion functions using Eqs. (12)–(17) and the constraint relations Eqs. (18)–(21). Therefore, the truncated lateral boundary conditions can also be expressed in terms of the lowest order expansion functions. In fact, the lateral boundary conditions written in terms of the lowest order expansion functions constitute the set

of micropolar cylinder equations and different order equations are obtained by different order truncations. The present method of deriving micropolar cylinder equations always renders hyperbolic equations. Moreover, the lateral boundary conditions are always fulfilled regardless of the truncation order. The set of micropolar cylinder equations may be reduced to a single equation in any of the lowest order expansion functions. The reduced single equation will have differential order of $6(N-1)$ for $m=0$ and $12N-8$ for $m>0$, which is readily seen when eliminating within the set of cylinder equations.

These sets of cylinder equations may also be obtained by using variational calculus. This is accomplished by adopting a generalized Hamilton's principle where the stresses, couple stresses, displacements and micro-rotations are varied simultaneously and independently [30, 31]. Variational calculus is also used to deduce the end boundary conditions in a consistent manner, see Section 4.2.

Explicit expressions for dynamic cylinder equations for the low order case $N=2$ are presented in Appendix C.1 for axisymmetric and Appendix C.2 for torsional motion, while the more complicated case for flexural motion is left out.

4.2. End boundary conditions

The end boundary conditions at $z=\{0,L\}$ must be derived trough the process of variational calculus [31]. The derivation of the end boundary conditions are not discussed in the present work, only the main conclusions are presented in order to understand the general concept. For each point at the end surfaces of the cylinder, one of the fields for each pair of the six pairs $\{u,t_{zr}\}$, $\{v,t_{z\theta}\}$, $\{w,t_{zz}\}$, $\{\phi,m_{zr}\}$, $\{\chi,m_{z\theta}\}$ and $\{\psi,m_{zz}\}$ is to be given. In total twelve fields must be chosen, six for each end. As discussed in Section 4.1 the cylinder equations are divided into two categories, $m=0$ and $m>0$. For the case of $m=0$, the decoupled axisymmetric and torsional modes are each of differential order $6(N-1)$, where N is the order of truncation. Hence $3(N-1)$ conditions are needed for each end to uniquely determine the motion for either axisymmetric or torsional modes. Consequently, $N-1$ boundary conditions must be derived from each of the three chosen end fields. For the case of $m>0$, the differential order of the cylinder equations is $12N-8$. As mentioned before six fields are to be given at each end. Hence,

N boundary conditions for the cylinder equations are obtained from each end field, resulting in $12N$ boundary conditions in total. This seems to result in an over determined system. However due to the constraints Eqs. (18)–(21) eight of the $12N$ stated boundary conditions, four from each end, are rendered redundant. The redundant conditions become linear combinations of other boundary conditions. Consequently, $12N - 8$ boundary conditions can be obtained.

The derivation procedure of the end boundary conditions is illustrated for one special case. Consider $m > 0$ where the end $z = L$ is subjected to the prescribed radial displacement field $u = \hat{u}$. As discussed previously, N boundary conditions are to be obtained from this particular end condition. By using Eq. (9), the radial displacement u is expanded in the following expansion functions $\{u_{m-1,m}, u_{m+1,m}, \ldots, u_{m+2N-1,m}\}$ consisting of N expansion functions. Based on variational calculus, the given function $\hat{u}$ is expanded as a cosine series in the circumferential variable and as a generalized radial Fourier series in terms of Zernike polynomials $R^{m-1}_{m+2i-1}(r/a)$ [31, 33]

$$\sum_{i=0}^{N} \hat{u}_{R,\{m+2i-1,m\}}(t) R^{m-1}_{m+2i-1}(r/a) = \sum_{i=0}^{N} \hat{u}_{\{m+2i-1,m\}}(t) r^{m+2i-1}. \tag{22}$$

The second index, m, of $\hat{u}_{\{m+2i-1,m\}}$ indicate the particular studied Fourier mode, $m > 0$. By simply equating the expansion functions of u with the expansion coefficients of $\hat{u}$ in Eq. (22), the set of N boundary conditions are obtained

$$u_{m+2i-1,m}(z = L, t) = \hat{u}_{\{m+2i-1,m\}}(t), \quad i = 0, 1, 2, \ldots, N. \tag{23}$$

The discussed procedure for obtaining boundary conditions for the cylinder equation through the end conditions is valid for other types of end conditions, e.g. micro-rotations, stresses and couple stresses.

5. Numerical results

This section concentrates on presenting numerical results for axisymmetric motion, $m = 0$, torsional motion, $m = 0$, and transverse flexural motion $m = 1$. The presented results constitute eigenfrequencies for three different end conditions, mode shapes of displacements, micro-rotations and stresses

and also a convergence study of the mode shapes. Since an analytical solution is not obtainable or very complicated even for the simplest of cases, higher order truncations will be used as benchmark solutions. The studied material is aluminium [34], where the material parameters are $E = 70.85$ GPa, $\nu = 0.33$, $\rho = 2800$ kg/m^3, $j = 0.325 \times 10^{-7}$ m^2, $\kappa = 1.31549 \times 10^{-5}$ GPa, $\alpha = 1.23552$ kN, $\beta = 0.1585$ kN, $\gamma = 0.59664$ kN. Note that the stress Eq. (5) is approximately symmetric due to the magnitude difference between μ and κ. All cylinders considered are traction free at the lateral surface, $r = a$.

5.1. Eigenfrequencies

In this section, the eigenfrequencies for the cases of axisymmetric motion, $m = 0$, torsional motion, $m = 0$, and transverse flexural motion $m = 1$, are studied for four different configurations of end conditions: simply supported, clamped and free at both ends and the case of one end is clamped while the other is free. The eigenfrequencies are normalized according to $\Omega = \omega a/c$ and $c = \sqrt{(\mu + \kappa)/\rho}$. If nothing else is stated, the highest presented truncation order has converged. Note that for the special case of classic elasticity theory, the results from the present work are in correspondence to the ones presented in [30, 31] as well as benchmark results reported elsewhere.

5.1.1. Axisymmetric motion

Firstly, consider the case for axisymmetric motion where both ends are simply supported. The simply supported end condition is stated as $w = \chi = 0$ and $t_{zr} = 0$ at $z = \{0, L\}$. The computed eigenfrequencies Ω_{pq} are numbered such that the first index corresponds to the mode shapes and the second index is the number of the particular eigenfrequency. The five eigenfrequencies with smallest magnitude for $L/a = 10$ and $L/a = 2$ are presented in Table 1. It is apparent that the eigenfrequencies of the cylinder equations converge as the truncation order is increased. The converged results are assumed to be exact, i.e. they are identical to the eigenfrequencies obtained by the complete three dimensional theory. As expected the more slender cylinder $L/a = 10$ converges faster in all cases, though the results of thicker cylinder are generally quite accurate. For the thicker cylinder all eigenfrequencies have converged except for Ω_{31}, which has a converged value of 4.6550.

L/a	Ω_{pq}	$N=2$	$N=4$	$N=6$	$N=8$
	Ω_{11}	0.51020	0.51098	0.51098	0.51098
	Ω_{12}	1.3612	1.4706	1.4711	1.4711
10	Ω_{21}	1.0069	1.0131	1.0131	1.0131
	Ω_{22}	1.4342	1.5384	1.5389	1.5389
	Ω_{31}	1.4742	1.4952	1.4952	1.4952
	Ω_{11}	2.2478	2.3282	2.3288	2.3288
	Ω_{12}	3.2833	3.3301	3.3303	3.3303
2	Ω_{21}	3.2094	3.5043	3.5075	3.5075
	Ω_{22}	3.9852	4.0239	4.0241	4.0241
	Ω_{31}	3.8064	4.5856	4.6531	4.6549

Table 1: The eigenfrequencies Ω_{pq} for $L/a = 10$ and $L/a = 2$ using theories of orders $N = 2, 4, 6, 8$ for axisymmetric mode, $m = 0$, of a simply supported cylinder.

Next, consider again the case of axisymmetric motion but where the end conditions are either clamped or free at both ends, and the case where one end is clamped and the other is free. The end conditions for the clamped end are stated as: $u = w = \chi = 0$, while for the free end the end conditions are $t_{zz} = t_{zr} = m_{z\theta} = 0$. The three lowest eigenfrequencies for the three cases are presented in Table 2 for $L/a = 10$. Here the converged higher order theory of $N = 16$ is also included due to the slower convergence. By studying the eigenfrequencies, it is seen that there are two types of convergence patterns; in most cases there are monotone convergence from below while a few has a more oscillating convergence pattern. The oscillating feature is seen for some cases with a clamped end, while the monotone convergence is seen for the simply supported as well as free ends. This sort of convergence behavior is also seen for the $m = 1$ cases below. Note that an oscillating behavior also occurred for the classic elastic case [30, 31]. Examining the three presented cases in Table 2, it is concluded that the free cylinder converges faster than the clamped case in accordance with previous work [31]. The case of clamped-free exhibits convergence patterns from both the clamped and the free cylinder, although the clamped-free cylinder converges faster than the wholly clamped cylinder.

BC	Ω_p	$N=2$	$N=4$	$N=6$	$N=8$	$N=16$
	Ω_1	0.5162	0.5154	0.5162	0.5166	0.5171
CC	Ω_2	1.020	1.023	1.024	1.025	1.026
	Ω_3	1.361	1.471	1.471	1.471	1.471
	Ω_1	0.5102	0.5110	0.5110	0.5110	0.5110
FF	Ω_2	1.007	1.013	1.013	1.013	1.013
	Ω_3	1.331	1.469	1.470	1.471	1.471
	Ω_1	0.2574	0.2571	0.2573	0.2574	0.2575
CF	Ω_2	0.7657	0.7671	0.7677	0.7681	0.7685
	Ω_3	1.253	1.264	1.265	1.265	1.266

Table 2: The eigenfrequencies for $L/a = 10$ using theories of orders $N = 2, 4, 6, 8, 16$ for axisymmetric mode, $m = 0$, of a cylinder subjected to clamped or free ends.

5.1.2. Torsional motion

The cases studied for axisymmetric motion are also considered for torsional motion. Here the simply supported end condition is stated as $v = \psi = 0$ and $m_{rr} = 0$ at $z = \{0, L\}$, while the clamped and free end conditions are stated by $v = \phi = \psi = 0$ and $t_{r\theta} = m_{rr} = m_{rz} = 0$, respectively at $z = \{0, L\}$. The eigenfrequencies for torsional motion are presented in Table 3 for the simply supported end conditions and Table 4 for the combination of clamped and free ends.

L/a	Ω_{pq}	$N=2$	$N=4$	$N=6$	$N=8$
	Ω_{11}	0.31416	0.31416	0.31416	0.31416
	Ω_{12}	0.64987	0.65008	0.65008	0.65008
10	Ω_{21}	0.62832	0.62832	0.62832	0.62832
	Ω_{22}	0.87728	0.87965	0.87965	0.87965
	Ω_{31}	0.94248	0.94248	0.94248	0.94248
	Ω_{11}	1.5708	1.5708	1.5708	1.5708
	Ω_{12}	3.1976	3.2147	3.2147	3.2147
2	Ω_{21}	3.1416	3.1416	3.1416	3.1416
	Ω_{22}	4.0287	4.0761	4.0766	4.0766
	Ω_{31}	4.7124	4.7124	4.7124	4.7124

Table 3: The eigenfrequencies Ω_{pq} for $L/a = 10$ and $L/a = 2$ using theories of orders $N = 2, 4, 6, 8$ for torsional mode, $m = 0$, of a simply supported cylinder.

BC	Ω_p	$N=2$	$N=4$	$N=6$	$N=8$	$N=16$
	Ω_1	0.3142	0.3142	0.3142	0.3142	0.3142
CC	Ω_2	0.6283	0.6283	0.6283	0.6283	0.6283
	Ω_3	0.6571	0.6551	0.6551	0.6551	0.6551
	Ω_1	0.3142	0.3142	0.3142	0.3142	0.3142
FF	Ω_2	0.6283	0.6283	0.6283	0.6283	0.6283
	Ω_3	0.6498	0.6500	0.6500	0.6500	0.6500
	Ω_1	0.1571	0.1571	0.1571	0.1571	0.1571
CF	Ω_2	0.4712	0.4712	0.4712	0.4712	0.4712
	Ω_3	0.5786	0.5783	0.5783	0.5783	0.5783

Table 4: The eigenfrequencies for $L/a = 10$ using theories of orders $N = 2, 4, 6, 8, 16$ for torsional mode, $m = 0$, of a cylinder subjected to clamped or free ends.

The eigenfrequencies for torsional motion generally converge faster than the axisymmetric case, and the rate of convergence is also faster than the transverse flexural case presented below. Many of the eigenfrequencies are rational multiples of π, as predicted in classical elasticity theory. However, certain eigenfrequencies that are due to the introduction of microstructure are captured using the micropolar theory as a basis for the approximate equations.

5.1.3. Flexural motion

Considering the third case of transverse flexural motion, $m = 1$, results similar to the previous cases are obtained. The simply supported end condition is stated by $u = v = \psi = 0$ and $t_{zz} = m_{zr} = m_{z\theta} = 0$ at $z = \{0, L\}$. For the clamped and free ends, the end conditions are stated as $u = v = w = \phi = \chi = \psi = 0$ and $t_{zz} = t_{zr} = t_{z\theta} = m_{zz} = m_{zr} = m_{z\theta} = 0$, respectively. The results for the simply supported case is presented in Table 5, both for $L/a = 10$ and $L/a = 2$. As expected, the slender cylinder converges more rapidly than the thicker cylinder. Eigenfrequencies for cases where the end conditions are either clamped or free are presented in Table 6.

L/a	Ω_{pq}	$N = 2$	$N = 4$	$N = 6$	$N = 8$
	Ω_{11}	0.076474	0.076966	0.076966	0.076966
	Ω_{12}	0.60602	0.60602	0.60602	0.60602
10	Ω_{21}	0.27071	0.27610	0.27610	0.27610
	Ω_{22}	0.74724	0.74726	0.74726	0.74726
	Ω_{31}	0.52586	0.54366	0.54367	0.54367
	Ω_{11}	1.0951	1.1592	1.1593	1.1593
	Ω_{12}	2.6148	2.8716	2.8781	2.8781
2	Ω_{21}	2.4552	2.7617	2.7680	2.7680
	Ω_{22}	3.7659	3.7721	3.7722	3.7722
	Ω_{31}	3.4781	4.2901	4.3354	4.3364

Table 5: The eigenfrequencies Ω_{pq} for $L/a = 10$ and $L/a = 2$ using theories of orders $N = 2, 4, 6, 8$ for transverse flexural mode, $m = 1$, of a simply supported cylinder.

The results for the transverse flexural motion converges orderly to the assumed exact value as the truncation order is increased. Note that some eigenfrequencies related to a particular mode shape may not be captured when using classical elasticity theory, since these stem from the influence of the micro-dynamical effects of the micropolar elasticity theory.

BC	Ω_p	$N=2$	$N=4$	$N=6$	$N=8$	$N=16$
	Ω_1	0.1495	0.1541	0.1542	0.1543	0.1542
CC	Ω_2	0.3477	0.3638	0.3643	0.3643	0.3642
	Ω_3	0.5868	0.6055	0.6057	0.6058	0.6059
	Ω_1	0.1653	0.1664	0.1664	0.1664	0.1664
FF	Ω_2	0.3946	0.4026	0.4026	0.4026	0.4026
	Ω_3	0.5492	0.5509	0.5511	0.5512	0.5513
	Ω_1	0.02793	0.02806	0.02807	0.02807	0.02807
CF	Ω_2	0.1532	0.1563	0.1564	0.1564	0.1564
	Ω_3	0.3705	0.3829	0.3831	0.3832	0.3831

Table 6: The eigenfrequencies for $L/a = 10$ using theories of orders $N = 2, 4, 6, 8, 16$ for transverse flexural mode, $m = 1$, of a cylinder subjected to clamped or free ends.

5.2. Mode shapes, stress distributions and error estimate

In this section, both mode shapes and stress distributions are illustrated for the fundamental frequency of the transverse bending mode, $m = 1$, when $L/a = 10$ and the cylinder is simply supported. Here the circumferential position θ is chosen so that the trigonometric dependency $\{\cos\theta, \sin\theta\}$ is set to unity for each case. Furthermore, the eigenmodes are normalized so that the radial displacement u at $r = 0$ and $z = L/2$ is equal to unity.

In order to asses the validity of the mode shapes, a study of the dependency of the error in the displacement and micro-rotation on the truncation order is presented. Here a higher order, $N = 16$, truncation was used as benchmark since analytical solutions are not available. The error is defined as the root mean square of the difference between the benchmark solution and lower

order solutions. Essentially the root mean square error measures how fast the eigenmodes of the displacements and micro-rotations converge. In Figure 1 the root mean square error of the displacement and micro-rotation fields are presented. It is clearly seen that the error decreases rapidly as the truncation order is increased. Hence, it is concluded that the lowest truncation order $N = 2$ produces a sufficiently small error and therefore only $N = 2$ order theory is used when assessing mode shapes and stress distributions.

In Figures 2–5 mode shapes and stress distributions are presented as a function of the radius and for $z = 3L/4$. Here the stresses t_{rr} and t_{rz} in Figure 4 and the couple stress m_{rr} in Figure 5(a) all fulfill the lateral boundary condition at $r = a$. The fact that boundary conditions are fulfilled exactly for all orders N, wether it may be lateral or end conditions, is an important feature of the presented method. Note that the classic elastic field distributions are here quite similar in shape to the ones presented in Abadikhah and Folkow [31].

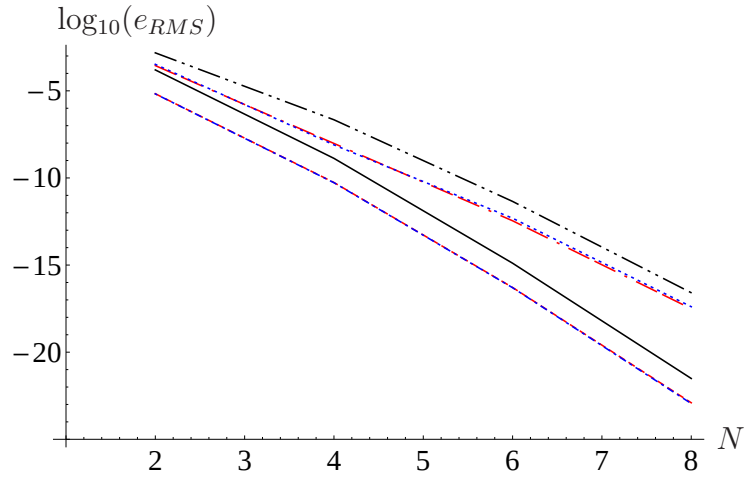

Figure 1: Root mean square error of displacements and micro-rotation as a function of truncation order N: - - - u, - · - v, —— w, – – · – – ϕ, · · · χ, – · · – ψ.

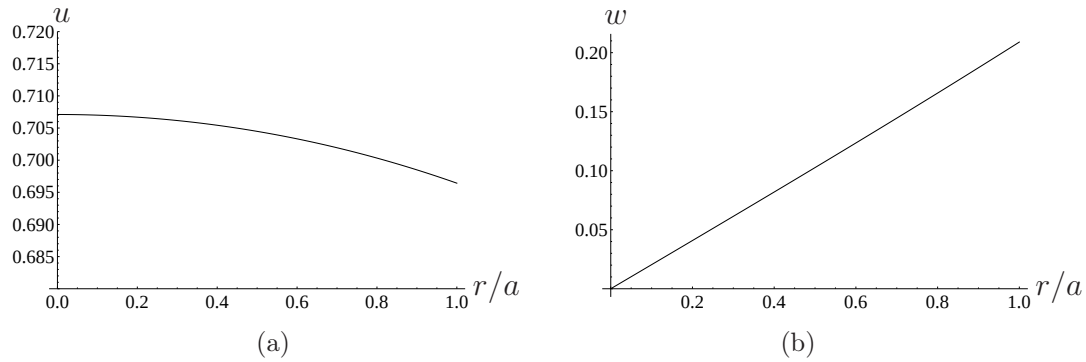

Figure 2: Radial (a) and longitudinal (b) displacement at $z = 3L/4$, for $N = 2$.

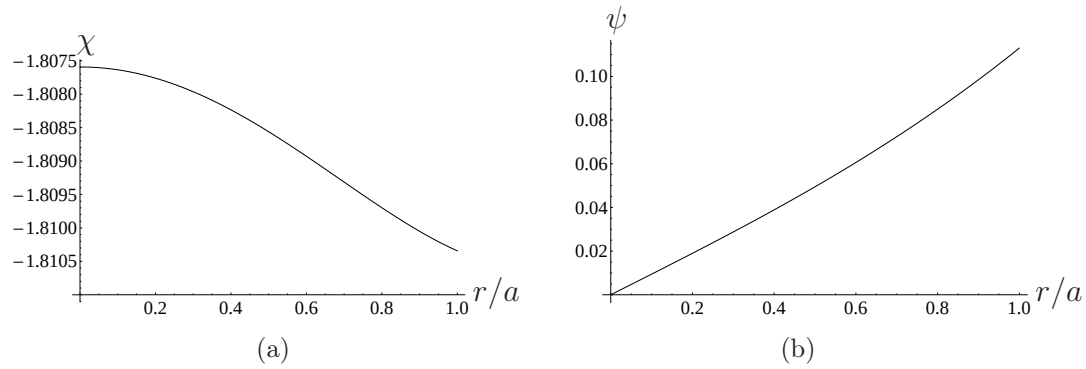

Figure 3: Circumferential (a) and longitudinal (b) micro-rotation at $z = 3L/4$, for $N = 2$.

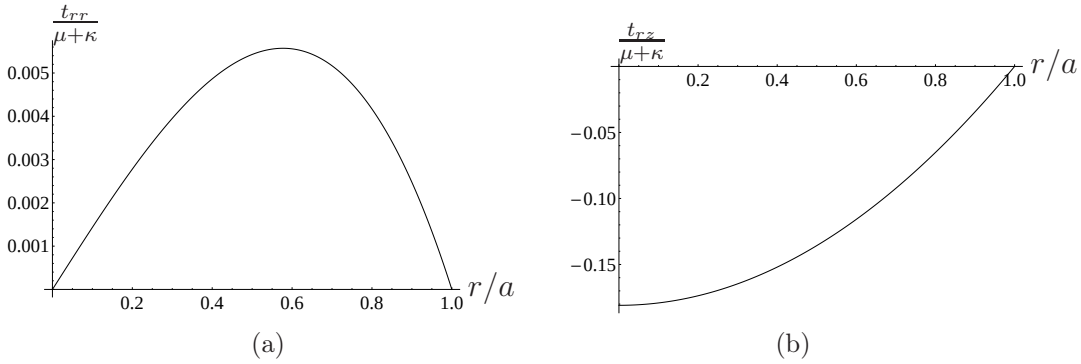

Figure 4: Normal stress t_{rr} (a) and shear stress t_{rz} (b) at $z = 3L/4$, for $N = 2$.

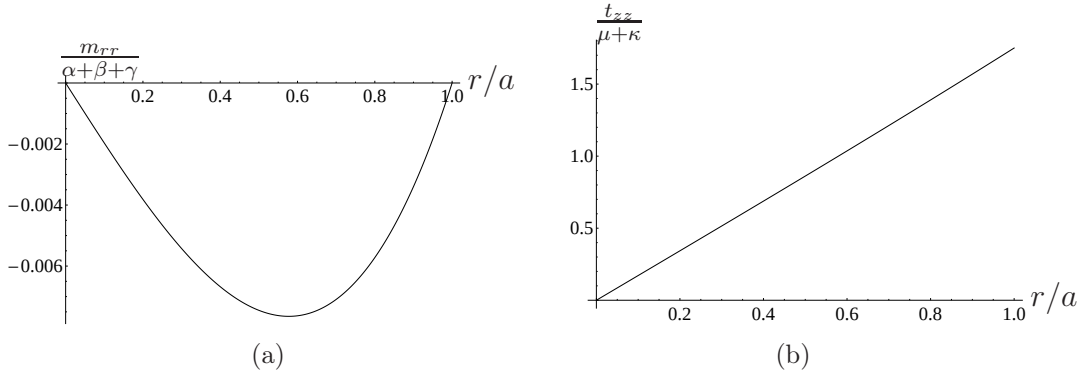

Figure 5: Normal couple stress m_{rr} (a) and normal stress t_{zz} (b) at $z = 3L/4$, for $N = 2$.

6. Conclusions

This work presents a systematic method for deriving variationally consistent approximate micropolar cylinder equations and corresponding boundary conditions to arbitrary order for different mode families. Numerical results are presented for an array of cases and various truncation orders. The lack of simple analytical solutions for the micropolar cylinder adds to the usefulness of the present equations. As the results illustrate, the present derivation method renders micropolar cylinder equations for axisymmetric, torsional and flexural motion in an efficient manner. Lateral and end boundary conditions are efficiently fulfilled for each mode and all truncation orders. The studied eigenfrequencies and eigenvalue modes converge in a stable manner,

where accurate results are obtained at a reasonably low order. Hence, the presented results show that these lower order cylinder equations can be efficiently used for the fundamental modes. As for higher order modes or less slender cylinders, higher order truncations are readily used. By increasing the truncation order, benchmark solutions to the three dimensional micropolar cylinder equations may be obtained. This is in line with the reported results using the present method for classical elastic structure cases [24, 28, 31].

Appendix A. Stresses

Each stress component expanded in the displacement and micro-rotation fields are expressed as (a prime denotes z-derivative):

$$t_{rr,\{k,m\}} = ((k+2)\lambda + (k+1)(2\mu+\kappa))u_{k+1,m} + m\lambda v_{k+1,m} + \lambda w'_{k,m}, \tag{A.1}$$

$$t_{\theta\theta,\{k,m\}} = ((k+2)\lambda + 2\mu + \kappa)u_{k+1,m} + m(\lambda+2\mu+\kappa)v_{k+1,m} + \lambda w'_{k,m}, \tag{A.2}$$

$$t_{zz,\{k,m\}} = (k+2)\lambda u_{k+1,m} + m\lambda v_{k+1,m} + (\lambda+2\mu+\kappa)w'_{k,m}, \tag{A.3}$$

$$t_{r\theta,\{k,m\}} = (k(\mu+\kappa)+\kappa)v_{k+1,m} - m\mu u_{k+1,m} - \kappa\psi_{k,m}, \tag{A.4}$$

$$t_{\theta r,\{k,m\}} = (k\mu-\kappa)v_{k+1,m} - m(\mu+\kappa)u_{k+1,m} + \kappa\psi_{k,m}, \tag{A.5}$$

$$t_{rz,\{k,m\}} = \mu u'_{k,m} + (k+1)(\mu+\kappa)w_{k+1,m} + \kappa\chi_{k,m}, \tag{A.6}$$

$$t_{zr,\{k,m\}} = (\mu+\kappa)u'_{k,m} + (k+1)\mu w_{k+1,m} - \kappa\chi_{k,m}, \tag{A.7}$$

$$t_{\theta z,\{k,m\}} = \mu v'_{k,m} - m(\mu+\kappa)w_{k+1,m} - \kappa\phi_{k,m}, \tag{A.8}$$

$$t_{z\theta,\{k,m\}} = (\mu+\kappa)v'_{k,m} - m\mu w_{k+1,m} + \kappa\phi_{k,m}, \tag{A.9}$$

$$m_{rr,\{k,m\}} = ((k+1)(\alpha+\beta+\gamma)+\alpha)\phi_{k+1,m} - m\alpha\chi_{k+1,m} + \alpha\psi'_{k,m}, \tag{A.10}$$

$$m_{\theta\theta,\{k,m\}} = ((k+2)\alpha+\beta+\gamma)\phi_{k+1,m} - m(\alpha+\beta+\gamma)\chi_{k+1,m} + \alpha\psi'_{k,m}, \tag{A.11}$$

$$m_{zz,\{k,m\}} = (k+2)\alpha\phi_{k+1,m} - m\alpha\chi_{k+1,m} + (\alpha+\beta+\gamma)\psi'_{k,m}, \tag{A.12}$$

$$m_{r\theta,\{k,m\}} = m\beta\phi_{k+1,m} + ((k+1)\gamma-\beta)\chi_{k+1,m}, \tag{A.13}$$

$$m_{\theta r,\{k,m\}} = m\gamma\phi_{k+1,m} + ((k+1)\beta-\gamma)\chi_{k+1,m}, \tag{A.14}$$

$$m_{rz,\{k,m\}} = \beta\phi'_{k,m} + (k+1)\gamma\psi_{k+1,m}, \tag{A.15}$$

$$m_{zr,\{k,m\}} = \gamma\phi'_{k,m} + (k+1)\beta\psi_{k+1,m}, \tag{A.16}$$

$$m_{\theta z,\{k,m\}} = \beta\chi'_{k,m} + m\gamma\psi_{k+1,m}, \tag{A.17}$$

$$m_{z\theta,\{k,m\}} = \gamma\chi'_{k,m} + m\beta\psi_{k+1,m}. \tag{A.18}$$

Appendix B. Recursion relations

The six recursion operators $\{f_u, f_v, f_w, f_\phi, f_\chi, f_\psi\}$ are presented in its entirety

$$
\begin{aligned}
&f_u(u_{m+k,m}, v_{m+k,m}, w_{m+k+1,m}, \phi_{m+k,m}, \chi_{m+k,m}, \psi_{m+k+1,m}) = \\
&= [(k+1)(k+3)(2m+k+1)(2m+k+3)(\mu+\kappa)(\lambda+2\mu+\kappa)]^{-1} \\
&\big([(m+k+1)(m+k+3)(\mu+\kappa) - m^2(\lambda+2\mu+\kappa)](\rho\ddot{u}_{m+k,m} - (\mu+\kappa)u''_{m+k,m} + \kappa\chi'_{m+k,m} \\
&- m[(m+k+1)\lambda + (m+k-1)\mu - 2\kappa](\rho\ddot{v}_{m+k,m} - (\mu+\kappa)v''_{m+k,m} - \kappa\phi'_{m+k,m}) \\
&- (k+1)(m+k+3)(2m+k+1)(\mu+\kappa)(\lambda+\mu)w'_{m+k+1,m} \\
&- m(k+1)(2m+k+1)(\lambda+2\mu+\kappa)\kappa\psi_{m+k+1,m}\big),
\end{aligned}
\tag{B.1}
$$

$$
\begin{aligned}
&f_v(u_{m+k,m}, v_{m+k,m}, w_{m+k+1,m}, \phi_{m+k,m}, \chi_{m+k,m}, \psi_{m+k+1,m}) = \\
&= [(k+1)(k+3)(2m+k+1)(2m+k+3)(\mu+\kappa)(\lambda+2\mu+\kappa)]^{-1} \\
&\big(m[(m+k+3)\lambda + (m+k+5)\mu + 2\kappa](\rho\ddot{u}_{m+k,m} - (\mu+\kappa)u''_{m+k,m} + \kappa\chi'_{m+k,m}) \\
&+ [(m+k+1)(m+k+3)(\lambda+2\mu+\kappa) - m^2(\mu+\kappa)](\rho\ddot{v}_{m+k,m} - (\mu+\kappa)v''_{m+k,m} - \kappa\phi'_{m+k,} \\
&+ m(k+1)(2m+k+1)(\mu+\kappa)(\lambda+\mu)w'_{m+k+1,m} \\
&+ (k+1)(m+k+3)(2m+k+1)(\lambda+2\mu+\kappa)\kappa\psi_{m+k+1,m}\big),
\end{aligned}
\tag{B.2}
$$

$$
\begin{aligned}
&f_w(u_{m+k+1,m}, v_{m+k+1,m}, w_{m+k,m}, \phi_{m+k+1,m}, \chi_{m+k+1,m}) = \\
&= [((m+k+2)^2 - m^2)(\mu+\kappa)]^{-1} \\
&\big(\rho\ddot{w}_{m+k,m} - (\lambda+2\mu+\kappa)w''_{m+k,m} - (m+k+2)(\lambda+\mu)u'_{m+k+1,m} - m(\lambda+\mu)v'_{m+k+1,m} \\
&+ m\kappa\phi_{m+k+1,m} - (m+k+2)\kappa\chi_{m+k+1,m}\big),
\end{aligned}
\tag{B.3}
$$

$$
\begin{aligned}
&f_\phi(u_{m+k,m}, v_{m+k,m}, w_{m+k+1,m}, \phi_{m+k,m}, \chi_{m+k,m}, \psi_{m+k+1,m}) = \\
&= [(k+1)(k+3)(2m+k+1)(2m+k+3)(\alpha+\beta+\gamma)\gamma]^{-1} \\
&\big([(m+k+1)(m+k+3)\gamma - m^2(\alpha+\beta+\gamma)](\rho j\ddot{\phi}_{m+k,m} - \gamma\phi''_{m+k,m} + 2\kappa\phi_{m+k,m} + \kappa v'_{m+k,m} \\
&- m[2\gamma - (m+k+1)(\alpha+\beta)](\rho j\ddot{\chi}_{m+k,m} - \gamma\chi''_{m+k,m} + 2\kappa\chi_{m+k,m} - \kappa u'_{m+k,m}) \\
&- (k+1)(m+k+3)(2m+k+1)(\alpha+\beta)\gamma\psi'_{m+k+1,m} \\
&+ m(k+1)(2m+k+1)(\alpha+\beta+\gamma)\kappa w_{m+k+1,m}\big),
\end{aligned}
\tag{B.4}
$$

$$
\begin{aligned}
&f_\chi(u_{m+k,m}, v_{m+k,m}, w_{m+k+1,m}, \phi_{m+k,m}, \chi_{m+k,m}, \psi_{m+k+1,m}) = \\
&= [(k+1)(k+3)(2m+k+1)(2m+k+3)(\alpha+\beta+\gamma)\gamma]^{-1} \\
&\big([(m+k+1)(m+k+3)(\alpha+\beta+\gamma) - m^2\gamma](\rho j\ddot{\chi}_{m+k,m} - \gamma\chi''_{m+k,m} + 2\kappa\chi_{m+k,m} - \kappa u'_{m+k,m} \\
&- m[2\gamma + (m+k+3)(\alpha+\beta)](\rho j\ddot{\phi}_{m+k,m} - \gamma\phi''_{m+k,m} + 2\kappa\phi_{m+k,m} + \kappa v'_{m+k,m}) \\
&- m(k+1)(2m+k+1)(\alpha+\beta)\gamma\psi'_{m+k+1,m} \\
&+ (k+1)(m+k+3)(2m+k+1)(\alpha+\beta+\gamma)\kappa w_{m+k+1,m}\big),
\end{aligned}
\tag{B.5}
$$

$$
\begin{aligned}
&f_\psi(u_{m+k+1,m}, v_{m+k+1,m}, \phi_{m+k+1,m}, \chi_{m+k+1,m}, \psi_{m+k,m}) = \\
&= [((m+k+2)^2 - m^2)\gamma)]^{-1} \\
&\big(\rho j\ddot{\psi}_{m+k,m} - (\alpha+\beta+\gamma)\psi''_{m+k,m} + 2\kappa\psi_{m+k,m} - (m+k+2)(\alpha+\beta)\phi'_{m+k+1,m} \\
&+ m(\alpha+\beta)\chi'_{m+k+1,m} - m\kappa u_{m+k+1,m} - (m+k+2)\kappa v_{m+k+1,m}\big).
\end{aligned}
\tag{B.6}
$$

Again a prime denotes z-derivative while a dot denotes time derivative.

Appendix C. Cylinder equations

The equations of motion for cylinders that are traction free at the lateral surface are given for $N = 2$. This is accomplished by adopting the procedure outlined in Section 3.2–3.3, using the expressions for the series terms Appendix A and the recursion relations Appendix B.

Appendix C.1. Axisymmetric motion

The set of three equations become $t_{rr,\{0,0\}} + a^2 t_{rr,\{2,0\}} = 0$, $m_{r\theta,\{0,0\}} + a^2 m_{r\theta,\{2,0\}} = 0$ and $t_{rz,\{0,0\}} = 0$. By adopting Eqs. (A.1), (A.6) and (A.13)

the equations are (the index $m = 0$ is here suppressed)

$$\begin{aligned}
&\lambda w_0' + (2(\lambda+\mu)+\kappa)u_1 \\
&+ \frac{a^2}{8}\Big[\frac{2\mu(\lambda+3\mu)-\kappa(\lambda-3\mu)}{2(\mu+\kappa)(\lambda+2\mu+\kappa)}\left((\lambda+2\mu+\kappa)w_0''' - \rho\ddot{w}'_0\right) \\
&+ \frac{2\lambda\mu-\kappa(\lambda+6\mu)-3\kappa^2}{\mu+\kappa}u_1'' + \frac{4\lambda+6\mu+3\kappa}{\lambda+2\mu+\kappa}\rho\ddot{u}_1 \\
&+ \frac{3\kappa(2\mu+\kappa)}{\mu+\kappa}\chi_1'\Big] = 0,
\end{aligned} \tag{C.1}$$

$$\begin{aligned}
&16\gamma(\mu+\kappa)(\gamma-\beta)\chi_1 \\
&+ a^2(\beta-3\gamma)\Big[\kappa\left((\lambda+2\mu+\kappa)w_0'' - \rho\ddot{w}_0\right) + 2\kappa\left(\lambda+2\mu+\kappa\right)u_1' \\
&+ 2\left((\mu+\kappa)(\gamma\chi_1'' - \rho j\ddot{\chi}_1) - \kappa(2\mu+\kappa)\chi_1\right)\Big] = 0,
\end{aligned} \tag{C.2}$$

$$(\lambda+2\mu+\kappa)w_0'' - \rho\ddot{w}_0 + 2\lambda u_1' = 0. \tag{C.3}$$

These equations are reduced to two equations in the special case of classical elasticity theory; these are identical to the ones presented in [30].

Appendix C.2. Torsional motion

The set of three equations become $m_{rr,\{0,0\}} + a^2 m_{rr,\{2,0\}} = 0$, $t_{r\theta,\{0,0\}} + a^2 t_{r\theta,\{2,0\}} = 0$ and $m_{rz,\{0,0\}} = 0$. By adopting Eqs. (A.4), (A.10) and (A.15) the equations are (the index $m = 0$ is here suppressed)

$$\begin{aligned}
&\alpha\psi_0' + (2\alpha+\beta+\gamma)\phi_1 \\
&+ \frac{a^2}{8}\Big[\frac{3\beta(\alpha+\beta+\gamma)-\alpha\gamma}{2\gamma(\alpha+\beta+\gamma)}\left((\alpha+\beta+\gamma)\psi_0''' - \rho j\ddot{\psi}'_0 - 2\kappa\psi_0'\right) \\
&+ \frac{3\beta(\alpha+\beta)-\gamma(\alpha+3\gamma)}{\gamma}\phi_1'' + \frac{4\alpha+3(\beta+\gamma)}{\alpha+\beta+\gamma}\rho j\ddot{\phi}_1 + \frac{2\kappa(4\alpha+3(\beta+\gamma))}{\alpha+\beta+\gamma}\phi_1 \\
&+ \frac{3\kappa(\beta+\gamma)}{\gamma}v_1'\Big] = 0,
\end{aligned} \tag{C.4}$$

$$
\begin{aligned}
&16\kappa\gamma(\mu+\kappa)(v_1-\psi_0)\\
&+a^2\Big[\kappa(2\mu+\kappa)\left((\alpha+\beta+\gamma)\psi_0''-\rho j\ddot{\psi}_0\right)-2\kappa\psi_0\Big)\\
&+2\kappa\left(2\mu(\alpha+\beta-\gamma)+\kappa(\alpha+\beta-3\gamma)\right)\phi_1'\\
&+2\left(\kappa^2(2\mu+\kappa)v_1-\gamma(2\mu+3\kappa)\left((\mu+\kappa)v_1''-\rho\ddot{v}_1\right)\right)\Big]=0,
\end{aligned}
\tag{C.5}
$$

$$
(\alpha+\beta+\gamma)\psi_0''-\rho j\ddot{\psi}_0-2\kappa\psi_0+2\alpha\phi_1'+2\kappa v_1=0. \tag{C.6}
$$

These equations are reduced to one equation in the special case of classical elasticity theory; this is identical to the one presented in [31].

References

[1] E. Cosserat, F. Cosserat, Théorie des Corps Déformables, A. Herman et Fils, Paris, 1906.

[2] A.C. Eringen, Microcontinuum Field Theory. I. Foundations and Solids, Springer, New York, 1999.

[3] D. Ieşan, Torsion of micropolar elastic beams, Int. J. Engng. Sci. 9 (1971) 1047–1060.

[4] G.V. Krishna Reddy, N.K. Venkatasubramanian, Saint-Venant's problem for a micropolar elastic circular cylinder, Int. J. Engng. Sci. 14 (1976) 1047–1057.

[5] G.V. Krishna Reddy, N.K. Venkatasubramanian, On the flexural rigidity of a micropolar elastic circular cylindrical tube, Int. J. Engng. Sci. 17 (1979) 1015–1021.

[6] A. Taliercio, D. Veber, Some problems of linear elasticity for cylinders in micropolar orthotropic material, Int. J. Solids Struct. 46 (2009) 3948–3963.

[7] A. Taliercio, D. Veber, Torsion of elastic anisotropic micropolar cylindrical bars, Eur. J. Mech. A Solids 55 (2016) 45–56.

[8] F.-Y. Huang, B.-H. Yan, J.-L. Yan, D.-U. Yang, Bending analysis of micropolar elastic beam using a 3-D finite element method, Int. J. Engng. Sci. 38 (2000) 275–286.

[9] D. Ieşan, Chiral effects in uniformly loaded rods, J. Mech. Phys. Solids 58 (2010) 1272–1285.

[10] S.L. Lakes, R.L. Benedict, Noncentrosymmetry in micropolar elasticity, Int. J. Engng. Sci. 20 (1982) 1161–1167.

[11] A.C. Smith, Torsion and vibrations of cylinders of a micropolar elastic solid, in: A.C. Eringen (Ed.) Recent Adv. Engng. Sci. 5, Gordon & Breach, London, 1970, pp. 129–137.

[12] A.J. Willson, The micropolar elastic vibrations of a cylinder, Int. J. Engng. Sci. 10 (1972) 17–22.

[13] R.Y. Vasudeva, R.K. Bhaskara, On wave propagation in a micropolar elastic cylinder, Int. J. Engng. Sci. 16 (1978) 299–302.

[14] R.K. Bhaskara, R.Y. Vasudeva, On flexural vibrations of micropolar elastic cylinders, Int. J. Engng. Sci. 24 (1986) 1397–1404.

[15] M. Marin, D. Baleanu, On vibrations in thermoelasticity without energy dissipation for micropolar bodies, Bound. Value Probl. 111 (2016) 1–19.

[16] S. Hassanpour, G.P. Heppler, Comprehensive and easy-to-use torsion and bending theories for micropolar beams, Int. J. Mech. Sci. 114 (2016) 71–87.

[17] S. Ramezani, R. Naghdabadi, S. Sohrabpour, Analysis of micropolar elastic beams, Eur. J. Mech. A Solids 28 (2009) 202–208.

[18] S. Shaw, High frequency vibration of a rectangular micropolar beam: A dynamical analysis, Int. J. Mech. Sci. 108-109 (2016) 83–89.

[19] I. Aganović, J. Tambača, Z. Tutek, Derivation and justification of the models of rods and plates from linearized three-dimensional micropolar elasticity, J. Elast. 84 (2006) 131–152.

[20] S.R. Chowdhury, Md.M. Rahaman, D. Roy, N. Sundaram, A micropolar periodynamic theory in linear elasticity, Int. J. Solids Struct. 59 (2015) 171–182.

[21] A. Boström, G. Johansson, P. Olsson, On the rational derivation of a hierarchy of dynamic equations for a homogeneous, isotropic, elastic plate, Int. J. Solids Struct. 38 (2001) 2487–2501.

[22] K. Mauritsson, P.D. Folkow, A. Boström, Dynamic equations for a fully anisotropic elastic plate, J. Sound Vib. 330 (2011) 2640–2654.

[23] P.D. Folkow, M. Johansson, Dynamic equations for fluid-loaded porous plates using approximate boundary conditions, J. Acoust. Soc. Am. 125 (2009) 2954–2966.

[24] S.S. Vel, R.C. Batra, Three-dimensional exact solution for the vibration of functionally graded rectangular plates, J. Sound Vib. 272 (2004) 703–730.

[25] H. Abadikhah, P.D. Folkow, A hierarchy of dynamic equations for micropolar plates, J. Sound Vib. 357 (2015) 427–436.

[26] H. Abadikhah, P.D. Folkow, A rational derivation of dynamic higher order equations for functionally graded micropolar plates, Compos. Struct. 153 (2016) 234–241.

[27] A.M. Hägglund, P.D. Folkow, Dynamic cylindrical shell equations by power series expansions, Int. J. Solids Struct. 45 (2008) 4509–4522.

[28] S.S. Vel, Exact elasticity solution for the vibration of functionally graded anisotropic cylindrical shells, Compos. Struct. 92 (2010) 2712–2727.

[29] A. Boström, On wave equations for elastic rods, Z. Angew. Math. Mech. 80 (2000) 245–251.

[30] P.D. Folkow, K. Mauritsson, Dynamic higher-order equations for finite rods, Q. Jl Mech. Appl. Math. 63 (2010) 1–22.

[31] H. Abadikhah, P.D. Folkow, A hierarchy of dynamic equations for solid isotropic circular cylinders, Wave Motion 51 (2014) 206–221.

[32] J.D. Achenbach, Wave Propagation in Elastic Solidss, North-Holland, Amsterdam, 1973.

[33] M. Born, E. Wolf, Principles of Optics, Cambridge University Press, Cambridge, 1999.

[34] A. Kiris, E. Inan, On the identification of microstretch elastic moduli of materials by using data on plates, Int. J. Eng. Sci. 46 (2008) 585–597.